# Photoinduced Electron Transfer and Enhanced Triplet Yields in Benzo[a]pyrene Derivative–Nucleic Acid Complexes and Covalent Adducts

**Vladimir Ya. Shafirovich,[§] Peter P. Levin,[⊥] Vladimir A. Kuzmin,[⊥] Thorgeir E. Thorgeirsson,[‡] David S. Kliger,[‡] and Nicholas E. Geacintov*,[†]**

*Contribution from the Chemistry Department and Radiation and Solid State Laboratory, New York University, New York, New York 10003, and Department of Chemistry and Biochemistry, University of California, Santa Cruz, California 95064*

*Received August 24, 1993. Revised Manuscript Received October 28, 1993[⊗]*

**Abstract:** The carcinogenic and mutagenic benzo[a]pyrenediol epoxide derivative 7*r*,8*t*-dihydroxy-9*t*,10*t*-epoxy-7,8,9,-10-tetrahydrobenzo[a] pyrene (BPDE) binds via its C-10 position predominantly to the exocyclic amino group of guanine residues in native DNA. In such DNA adducts, the fluorescence of the pyrenyl moieties is strongly quenched by physicochemical interaction with the DNA bases. Using nanosecond time scale transient absorption techniques, products of the fluorescence quenching have been examined in two model systems in aqueous and polar organic solvents. The first is a monomeric, covalently linked (+)-*trans*-BPDE-N²-2′-deoxyguanosine adduct (BPDE–dG), the most abundant adduct when (+)-BPDE binds to native DNA; the second consists of mixtures of 7,8,9,10-tetrahydroxytetrahydrobenzo[a]pyrene (BPT) with dG, which was used to study the role of noncovalent interactions in solvents of different hydrophobicities. At moderate laser pulse energies (≤25 mJ/cm²/pulse, 347 nm), the primary products of the fluorescence quenching reaction are pyrenyl residue triplet excited states, with greatly enhanced yields (by factors of 3–10 or more relative to the yields expected from simple intersystem crossing). The primary quenching reaction involves photoinduced electron transfer from dG to pyrenyl residues, followed by efficient recombination to form triplet excited states. Consistent with this mechanism, pyrenyl radical anions are observed in solutions of BPT and dG (0.1 M) in polar organic solvents. However, radical ions are not observed in any of the covalently linked adducts nor in aqueous solutions of BPT and dG on time scales > 10 ns; triplet excited states are unique products of the fluorescence quenching reaction. These effects are attributed to noncovalent fluorophore–dG interactions in aqueous BPT/dG solutions and to the close proximities of electron donor/acceptor pairs in the covalently linked systems. Both of these circumstances favor rapid ion pair recombination, limiting their escape into the bulk of the solution.

## 1. Introduction

Polycyclic aromatic hydrocarbons (PAHs), including the widely studied carcinogen benzo[a]pyrene, are metabolized to highly reactive diol epoxide derivatives[1] which bind covalently to native DNA.[2-4] It is well established[1] that the ultimate tumorigenic and mutagenic metabolite of the PAH compound benzo[a]pyrene, the metabolite 7,8-dihydroxy-9,10-epoxy-7,8,9,10-tetrahydrobenzo[a]pyrene (BPDE), binds to native DNA predominantly via addition of the exocyclic amino group (N2) of 2′-deoxyguanosine (dG) residues to the C-10 position of BPDE[2-4] (the structure of a BPDE–$N^2$-dG adduct with (+)-*trans* stereochemistry is depicted in Figure 1). Differences in adduct conformations[5-7] may be the basis for the differences in biological consequences associated with various benzo[a]pyrenediol epoxide stereoisomers. Two major types of adduct DNA binding sites, one intercalative and the other external, can be distinguished by UV absorbance,[5,8] circular dichroism,[8] NMR methods,[7] and fluorescence charac-

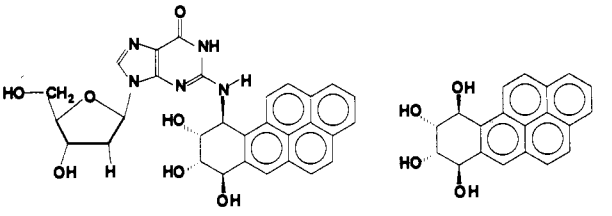


**Figure 1.** Molecular structure of (+)-*trans*-BPT (a racemic mixture of *trans*-BPT was used in this work) and the (+)-*trans*-BPDE–dG adduct.

* Corresponding author. TEL: (212) 998-8407. FAX: (212) 998-8421.
† New York University.
‡ University of California, Santa Cruz.
§ On leave from the Institute of Chemical Physics at Chernogolovka, Russian Academy of Sciences, Chernogolovka 142432, Russia.
⊥ On leave from the Institute of Chemical Physics, Russian Academy of Sciences, Moscow V-334, Russia.

⊗ Abstract published in *Advance ACS Abstracts*, December 15, 1993.

(1) For reviews, see, e.g.: (a) Conney, H. *Cancer Res.* **1982**, *42*, 4875. (b) Singer, B.; Grunberger, D. *Molecular Biology of Mutagens and Carcinogens;* Plenum Press: New York, 1983. (c) Harvey, R. G. *Polycyclic Aromatic Hydrocarbons: Chemistry and Carcinogenicity;* Cambridge University Press: Cambridge, UK, 1991.

(2) (a) Weinstein, I. B.; Jeffrey, A. M.; Jennette, K. W.; Blobstein, S. H.; Harvey, R. G.; Harris, C.; Autrup, H.; Kasal, H.; Nakanishi, K. *Science* **1976**, *193*, 592. (b) Jeffrey, A. M.; Jennette, K. W.; Blobstein, S. H.; Weinstein, I. B.; Beland, F. A.; Harvey, R. G.; Kasai, H.; Miura, I.; Nakanishi, K. *J. Am. Chem. Soc.* **1976**, *98*, 5714. (c) Koreeda, M.; Moore, P. D.; Yagi, H.; Yeh, H. J. C.; Jerina, D. M. *J. Am. Chem. Soc.* **1976**, *98*, 6720. (d) Nakanishi, K.; Kasai, H.; Cho, H.; Harvey, R. G.; Jeffrey, A. M.; Jennette, K. W.; Weinstein, I. B. *J. Am. Chem. Soc.* **1977**, *99*. 258. (e) Jeffrey, A. M.; Weinstein, I. B.; Jennette, K. W.; Grzeskowiak, K.; Nakanishi, K. *Nature* **1977**, *269*, 348. (f) Koreeda, M.; Moore, P. D.; Wislocki, P. G.; Levin, W.; Conney, A. H.; Yagi, H.; Jerina, D. M. *Science* **1978**, *199*, 778.

(3) Meehan, T.; Straub, K. *Nature* **1979**, *277*, 410.

(4) Cheng, S. C.; Hilton, B. D.; Roman, J. M.; Dipple, A. *Chem. Res. Toxicol.* **1989**, *2*, 334.

(5) (a) Geacintov, N. E. In *Polycyclic Aromatic Hydrocarbon Carcinogenesis: Structure-Activity Relationships;* Yang, S. K., Silverman, B. D., Eds.; CRC Press: Boca Raton, FL, 1988; Vol. II, p 181. (b) Gräslund, A.; Jernström, B. *Q. Rev. Biophys.* **1989**, *22*, 1.

(6) Singh, S. S.; Hingerty, B. E.; Singh, U. C.; Greenberg, J. P.; Geacintov, N. E.; Broyde, S. *Cancer Res.* **1991**, *51*, 3482.

(7) (a) Cosman, M.; de los Santos, C.; Fiala, R.; Hingerty, B. E.; Ibanez, V.; Margulis, L. A.; Live, D.; Geacintov, N. E.; Broyde, S.; Patel, D. J. *Proc. Natl. Acad. Sci. U.S.A.* **1992**, *89*, 1914. (b) de los Santos, C.; Cosman, M.; Hingerty, B. E.; Ibanez, V.; Margulis, L. A.; Geacintov, N. E.; Broyde, S.; Patel, D. J. *Biochemistry* **1992**, *31*, 5245. (c) Cosman, M.; de los Santos, C.; Fiala, R.; Hingerty, B. E.; Ibanez, V.; Luna, E.; Harvey; R. G.; Geacintov, N. E.; Broyde, S.; Patel, D. *Biochemistry* **1993**, *32*, 4145.

0002-7863/94/1516-0063$04.50/0 

teristics.[8,9] Fluorescence is a particularly sensitive analytical tool for detecting adducts in native DNA[10] and for studying physicochemical interactions between the bound PAH molecules and the DNA bases.[8,11] However, the fluorescence of various polynuclear aromatic fluorophores is strongly quenched upon binding to DNA[11,12] and by monomeric nucleic acid bases in solution.[13-15] In particular, the fluorescence of the pyrenyl aromatic chromophore in covalent BPDE–native DNA adducts[12] and in complexes derived from the noncovalent binding of the BPDE hydrolysis product 7,8,9,10-tetrahydroxytetrahydrobenzo[*a*]-pyrene (BPT, Figure 1) to native DNA[16] is strongly quenched. The quenching mechanism most likely involves photoinduced electron transfer from the guanine residues to pyrenyl moieties.[15,17] Previous work has shown that photoinduced electron transfer between photoexcited polycyclic aromatic hydrocarbons (or aromatic dyes) and nucleic acids is a viable fluorescence quenching mechanism.[18-20]

Photoirradiation of noncovalent polycyclic aromatic dye–DNA complexes[21] and covalent BPDE–native DNA adducts[22] can result in strand scission. It has been known for some time that guanine residues are the most easily oxidized of the nucleic acid bases.[23] Photoinduced electron-transfer reactions in aromatic dye– or PAH–DNA complexes or adducts may lead to the formation of the dG radical cation, which may play the key role (Mao, B.; Li, B.; Liu, T.-M.; Geacintov, N. E., manuscript in preparation) in initiating the complex series of chemical events leading to DNA strand scission.[24]

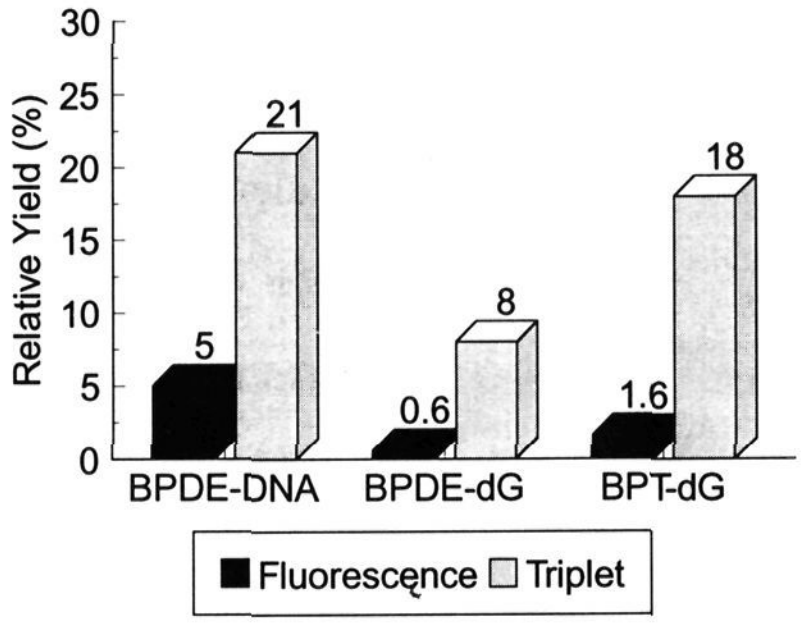


**Figure 2.** Fluorescence and triplet yields of a covalent BPDE–native DNA adduct, covalent (+)-*trans*-BPDE–dG adduct, and BPT and dG (0.028 M) aqueous solutions, relative to BPT in aqueous solution.

In an effort to characterize the fluorescence quenching mechanisms in noncovalent complexes and adducts derived from the binding of the important benzo[*a*]pyrene metabolites with DNA, we have used nanosecond laser transient absorption methods to investigate the nature of the products of the fluorescence quenching reactions. Because the fluorescence of covalent BPDE–native DNA adducts is heterogeneous in nature,[11e,f] we have focused our attention instead on two well-defined model systems in aqueous and nonaqueous solutions: (1) the covalently linked BPDE–dG adduct (Figure 1) and (2) quenching of the fluorescence of BPT by dG in which only noncovalent interactions between this electron-acceptor–donor pair can occur.[15] The first is a good model system because BPDE reacts predominantly with dG residues in native DNA to form (C10-BPDE)–($N^2$-dG) adducts.[2-4] The second system is of interest because the role of van der Waals hydrophobic interactions in fluorescence quenching can be conveniently examined by comparing the quenching characteristics in aqueous and non-aqueous polar solvents; in aqueous systems, the hydrophobic BPT–dG interactions leading to complex formation are favored,[15] while in organic solvents such interactions are greatly diminished. Indeed, preliminary studies have shown that the fluorescence yield of BPDE–dG adducts depends strongly on the polarity of the solvent.[17] Here, we show that the appearance of transient pyrenyl residue radical ions is solvent-dependent and also depends strongly on the energy of the 347-nm excitation laser pulse energies. In all cases, the major product of the fluorescence quenching reaction is the pyrenyl triplet excited state with a yield up to 1 order of magnitude or more greater than expected from a simple intersystem crossing mechanism from molecular singlet excited states (Figure 2). The enhancement in triplet yields suggests that the free energy stored in the primary fluorescence quenching products (exciplexes or singlet radical ion pairs) is greater than the energy of the pyrenyl triplet state. The mechanisms of fluorescence quenching in these pyrenyl residue–nucleic acid model systems resemble the electron-transfer mech-

(8) Geacintov, N. E.; Cosman, M.; Mao, B.; Alfano, A.; Ibanez, V.; Harvey, R. G. *Carcinogenesis* **1991**, *12*, 2099.

(9) (a) Kim, S. K.; Brenner, H. C.; Soh, B. J.; Geacintov, N. E. *Photochem. Photobiol.* **1989**, *50*, 327. (b) Jankowiak, R.; Lu, P.-Q.; Small, G. J. *Chem. Res. Toxicol.* **1990**, *3*, 39. (c) Lu, P.; Jeong, H.; Jankowiak, R.; Small, G. J. *Chem. Res. Toxicol.* **1991**, *4*, 58. (d) Zhao, R.; Liu, T.-M.; Kim, S.-K.; MacLeod, M. C.; Geacintov, N. E. *Carcinogenesis* **1992**, *13*, 1817. (e) Marsch, G. A.; Jankowiak, R.; Farhat, J. H.; Small, G. J. *Anal. Chem.* **1992**, *64*, 3038.

(10) (a) Jankowiak, R.; Cooper, R. S.; Zamzow, D.; Small, G. J.; Doskocil, G.; Jeffrey, A. M. *Chem. Res. Toxicol.* **1988**, *1*, 60. (b) Jankowiak, R.; Small, G. J. *Anal. Chem.* **1989**, *61*, 1023A. (c) Jankowiak, R.; Small, G. J. *Chem. Res. Toxicol.* **1991**, *4*, 259.

(11) (a) Shahbaz, M.; Harvey, R. G.; Prakash, A. S.; Boal, T. R.; Zegar, I. S.; LeBreton, P. R. *Biochem. Biophys. Res. Commun.* **1983**, *112*, 1. (b) Zegar, I. S.; Prakash, A. S.; LeBreton, P. R. *J. Biomol. Struct. Dyn.* **1984**, *2*, 531. (c) Abramovich, M.; Prakash, A. S.; Harvey, R. G.; Zegar, I. S.; LeBreton, P. R. *Chem. Biol. Interact.* **1985**, *55*, 39. (d) Zegar, I. S.; Prakash, A. S.; Harvey, R. G.; LeBreton, P. R. *J. Am. Chem. Soc.* **1985**, *107*, 7990. (e) Geacintov, N. E.; Zinger, D.; Ibanez, V.; Santella, R.; Grunberger, D.; Harvey, R. G. *Carcinogenesis* **1987**, *8*, 925. (f) Zinger, D.; Geacintov, N. E.; Harvey, R. G. *Biophys. Chem.* **1987**, *27*, 131. (g) Price, H. L.; Fetzer, S. M.; LeBreton, P. R. *Biochem. Biophys. Res. Commun.* **1990**, *168*, 1095. (h) Urano, S.; Price, H. L.; Fetzer, S. M.; Briedis, A. V.; Milliman, A.; LeBreton, P. R. *J. Am. Chem. Soc.* **1991**, *113*, 3881. (i) Eriksson, M.; Kim, S. K.; Sen, S.; Gräslund, A.; Jernström B.; Nordén, B. *J. Am. Chem. Soc.* **1993**, *115*, 1639.

(12) (a) Prusik, T.; Geacintov, N. E.; Tobiasz, C.; Ivanovic, V.; Weinstein, I. B. *Photochem. Photobiol.* **1979**, *29*, 223. (b) Hogan, M.; Dattagupta, N.; Whitlock, J. P., Jr. *J. Biol. Chem.* **1981**, *256*, 4504. (c) McLeod, M. C.; Mansfield, B. K.; Selkirk, J. K. *Carcinogenesis* **1982**, *3*, 1031. (d) Undeman, O.; Lycksell, P.-O.; Gräslund A.; Astlind, T.; Ehrenberg, A.; Jernström, B.; Tjernéld, F.; Nordén, B. *Cancer. Res.* **1983**, *43*, 1851. (e) Chen, F.-M. *J. Biomol. Struct. Dyn.* **1986**, *4*, 401. (f) Kim, S. K.; Geacintov, N. E.; Zinger, D.; Sutherland, J. C. In *Synchrotron Radiation in Structural Biology. Basic Life Sciences, Vol. 51;* Sweet, R. M., Woodhead, A. D., Eds.; Plenum Press: 1989; p 187.

(13) Geacintov, N. E.; Prusik, T.; Khosrofian, J. M. *J. Am. Chem. Soc.* **1976**, *98*, 6444.

(14) (a) Lianos, P.; Georghio, S. *Photochem.Photobiol.* **1979**, *29*, 13. (b) Dunn, D. A.; Lin, V. H.; Kochevar, I. E. *Photochem. Photobiol.* **1991**, *53*, 47.

(15) Geacintov, N. E.; Zhao, R.; Kuzmin, V. A.; Kim, S. K.; Pecora, L. J. *Photochem. Photobiol.* **1993**, *58*, 185.

(16) (a) Ibanez, V.; Geacintov, N. E.; Gagliano, A. G.; Brandimarte, S.; Harvey, R. G. *J. Am. Chem. Soc.* **1980**, *102*, 5661. (b) MacLeod, M. C.; Selkirk, J. K. *Carcinogenesis* **1982**, *3*, 287. (c) MacLeod, M. C.; Smith, B.; McClay, J. *J. Biol. Chem.* **1987**, *262*, 1081. (d) Geacintov, N. E.; Brenner, H. C. *Photochem. Photobiol.* **1989**, *50*, 841.

(17) (a) Margulis, L.; Pluzhnikov, P. F.; Mao, B.; Kuzmin, V. A.; Chang, Y. J.; Scott, T. M.; Geacintov, N. E. *Chem. Phys. Lett.* **1991**, *187*, 597. (b) Geacintov, N. E.; Mao, B.; France, L. L.; Zhao, R.; Chen, J.; Liu, T.-M.; Ya, N.-Q.; Margulis, L. A.; Sutherland, J. C. *Proc. SPIE: Time-Resolved Laser Spectroscopy in Biochemistry III* **1992**, *1640*, 774.

(18) (a) Löber, G.; Kitler, L. *Stud. Biophys.* **1978**, *73*, 25. (b) Kitler, L.; Löber, G.; Gollmock, F. A.; Berg, H. *Bioelectrochem. Bioenerg.* **1980**, *7*, 503. (c) Brun, A. M.; Harriman, A. *J. Am. Chem. Soc.* **1992**, *114*, 3656.

(19) Sharifian, H. A.; Pyun, C.-H.; Jiang, F.-B.; Park, S-M. *J. Photochem.* **1985**, *30*, 229.

(20) Seidel, C. *Proc. SPIE: Biomolecular Spectroscopy II* **1991**, *1432*, 91,

(21) Kochevar, I. E.; Dunn, D. A. In *Bioorganic Chemistry*; Morrison, H., Ed.; Wiley: New York, 1990; p 273.

(22) (a) Boles, T. C.; Hogan, M. E. *Biochemistry* **1986**, *25*, 3039. (b) Dittrich, K. A.; Krugh, T. R. *Chem. Res. Toxicol.* **1991**, *4*, 270.

(23) For a review purine radical chemistry, see: Steenken, S. *Chem. Rev.* **1989**, *89*, 503.

(24) (a) Schulte-Frohlinde, D. In *Mechanisms of DNA Damage and Repair. Implications for Carcinogenesis and Risk Assessment. Basic Life Sciences, Vol. 38;* Simic, M. G., Grossman, L., Upton, A. D., Eds.; Plenum Press: New York, 1986; p 19. (b) von Sonntag, C. *The Chemical Basis of Radiation Biology;* Francis and Taylor: London, 1987. (c) Symons, M. C. R. *J. Chem. Soc., Faraday Trans. 1*, **1987**, *83*, 1.

anisms occurring in the classical dimethylaniline–pyrene fluorophore donor–acceptor systems that have been extensively characterized in the pioneering studies of Mataga, Ottolenghi, Weller, Michel-Beyerle, and their co-workers.[25-29]

## 2. Experimental Section

The transient absorption spectra and decay kinetics were recorded using two laser flash photolysis systems. In the first system, a Q-switched Nd:Yag laser (Quanta Ray, DCR-2) using third harmonic light pulses was used (355 nm, 7-ns duration, energy 13 mJ/pulse, 3-mm-diameter spot). A xenon flashlamp (EG&G Q3CP-2) was used as the probe flash; the light transmitted by the sample was detected by means of an optical multichannel analyzer (OMA) detector system consisting of a Jarrell-Ash spectrograph (Monospec 25), a reticon detector (Princeton Applied Research Model 1420), and an OMA controller (Princeton Applied Research Model 1461). The output of this system was fed to an XT computer for calculation of the transient absorption spectra. The second laser flash photolysis system was based on a Q-switched ruby laser excitation system (Holobeam Series 300, second harmonic 347-nm operating wavelength, 10-ns pulse duration, energy ≤20 mJ/pulse, 5-mm-diameter beam). The kinetic spectrophotometer (~10-ns resolution) included a pulsed high-pressure Xenon arc lamp (100 W), an electromechanical shutter, a monochromator with different replaceable gratings (300–1000 nm), a Hamamatsu R 928 photomultiplier, and an averaging system consisting of a Gould Biomation 8100 wave form digitizer and a Model 4203 signal averager (Princeton Applied Research, Princeton, NJ) coupled to an IBM AT-386 computer.

Highly polymerized calf thymus DNA was obtained from Sigma Chemical Co. (St. Louis, MO) and purified by standard procedures.[30] Racemic BPDE was obtained from the National Cancer Institute Chemical Carcinogen Reference Standard Repository (8 mM solution in tetrahydrofuran containing 5% triethylamine as a stabilizer). The DNA was reacted with BPDE as previously described.[11e] The reaction mixture was extracted 10 times with ether and subsequently dialyzed 5 times for 12-h periods against the 5 mM sodium cocadylate buffer, pH 7, in order to remove the BPT hydrolysis products. The dialysis was carried out at 4 °C in the dark. The degree of covalent modification of DNA (covalently bound BPDE molecules/DNA nucleotide) was determined spectrophotometrically to be to 2.0 ± 0.2%. The extinction coefficients used were $\epsilon_{346}$ = 29 500 $cm^{-1}$ $M^{-1}$ for bound BPDE and $\epsilon_{258}$ = 6700 $cm^{-1}$ $M^{-1}$ for DNA. The modified DNA was characterized by a melting temperature of 69.5 °C and a hyperchromicity of 25 ± 2%.

The (+)-*trans* stereoisomeric BPDE–dG adduct (Figure 1) was synthesized and isolated by known methods[4] and was purified by HPLC techniques. A Waters Model 501 solvent delivery system with a Waters 990 Series photodiode array detector (Millipore Corp.) was used for this purpose, employing a 4.6 × 250.0 mm column Microsorb-MV (Rainin Instrument Company) and a 37–42% linear gradient of methanol in 20 mM sodium phosphate buffer, pH 7. The BPDE–dG adduct was eluted in 120 min (flow rate 1 mL/min, UV detection of the product at 345 nm). The circular dichroism spectra of the BPDE–dG adduct were consistent with those published by Cheng et al. for the (+)-*trans*-BPDE-$N^2$-dG isomer.[4]

The BPT was prepared by hydrolysis of racemic BPDE in aqueous solution.[16a] The racemic *trans* product,[31] used throughout this work, was isolated from the *cis* product by reverse-phase HPLC. A Model L-6200 intelligent pump (Hitachi Instruments) was used for this purpose, employing a 10- × 250.0-mm Hypersil-ODS column (Keystone Scientific) and a 55–65% linear gradient of methanol in 20 mM sodium phosphate buffer, pH 7, in 60 min (flow rate 3 mL/min, UV detection of product at 254 nm).

Spectrophotometric grade acetonitrile, *N,N'*-dimethylformamide (DMF), and *N*-methylformamide (NMF), reagent grade *N,N'*-dimethylaniline (DMA), and tetracyanoethylene from Aldrich were used without further purification. The nucleoside dG (Sigma) was purified by G-10 Sephadex column chromatography as necessary (the necessity of removing impurities was assessed by comparing the efficiency of quenching of the fluorescence of BPT by highly purified and unpurified dG).

Sample concentrations (pyrenyl chromophores) were 10–30 (nanosecond laser flash photolysis) or 0.5–5 μM (absorption and fluorescence measurements). Before all laser flash photolysis and fluorescence studies, the cells were carefully flushed with argon to remove $O_2$. All measurements were conducted at 23 ± 1 °C. In our experiments, the BPT and BPDE–dG model systems were photochemically stable enough to allow for repeated laser flash photolysis experiments without a flow system. However, extensive laser flash excitation of BPDE–native DNA adducts resulted in the formation of free BPT,[11f] which was easily monitored via its extensive fluorescence yield.[11e] Therefore, all measurements with BPDE–DNA solutions were restricted to the first 1–2 laser flashes; under these conditions, adduct decomposition did not exceed 1–2%.

## 3. Results

**3.1. General Aspects. Absorption and Fluorescence Characteristics in Aqueous and Polar Organic Solvents.** In order to study the effects of hydrophobic interactions between the pyrenyl and nucleic acid residues on fluorescence quenching phenomena, the fluorescence and transient absorption characteristics of the covalent BPDE–dG adducts and BPT + dG (noncovalent interactions only) in water and in solutions of the polar organic solvents DMF and NMF were studied. The solubility of dG in these organic solvents (~0.2 M) is sufficiently high for the purposes of these studies; the polar solvent acetonitrile has traditionally been employed to study pyrene photochemistry;[25] however, the solubility of dG in this solvent is inadequate (≤$10^{-3}$ M). While no significant differences in the molar extinction coefficients[32] of BPT were observed in water, DMF, and NMF, the absorption maxima occur at somewhat different wavelengths ($\lambda_{max}$ = 343 nm in water and acetonitrile; $\lambda_{max}$ = 345 nm in DMF and NMF). The absorption spectra of BPT are unchanged in DMF and NMF solutions as a function of dG concentration up to 0.2 M. The observed absorption spectra are equal to the sum of spectra of the individual component chromophores, and thus neutral complex formation (BPT···dG) or charge-transfer complex formation can be ignored in these polar organic solvents.

In aqueous solutions, however, addition of dG (≤0.01 M) results in pronounced shifts of the BPT absorption bands in the 300–350-nm region to longer wavelengths because of BPT···dG ground-state complex formation:[15]

$$\mathrm{BPT} + \mathrm{dG} \overset{K_g}{\rightleftharpoons} (\mathrm{BPT}\cdots\mathrm{dG}) \qquad (1)$$

where $K_g$ is the ground-state complex equilibrium constant. We continued to observe well-defined isobestic points at 321, 330, 336, and 346 nm in the entire range of dG concentrations in water up to 0.03 M. Therefore, no indication of a substantial formation of complexes with a stoichiometry higher than 1:1 is indicated in this concentration range.

The longest-wavelength absorption maximum of BPDE–dG adducts in aqueous solutions[2e] occurs at 345 nm and is thus red-shifted by 2 nm with respect to BPT; in DMF and NMF, the

(25) For a review of pyrene photochemistry, see: (a) Mataga, N. In *Electron Transfer in Inorganic, Organic, and Biological Systems:* Bolton, J. R., Mataga, N., McLendon, G., Eds.; American Chemical Society: Washington, DC, 1991. (b) Mataga, N. In *Molecular Interactions:* Ratajczak, H., Orville-Thomas, J., Eds.; Wiley: New York, 1981; Vol. II, pp 509–570. (c) Mataga, N.; Ottolenghi, M. In *Molecular Association Including Molecular Complex:* Foster, R., Ed.; Academic Press: New York, 1979; Vol. II, pp 1–78.

(26) (a) Orbach, N.; Ottolenghi, M. *Chem. Phys. Lett.* **1975**, *35*, 175. (b) Orbach, N.; Ottolenghi, M. In *The Exciplex:* Gordon, M., Ware, W. R., Eds.; Academic Press: New York, 1975; p 75.

(27) Masuhara, H.; Hino, T.; Mataga, N. *J. Phys. Chem.* **1975**, *79*, 994.

(28) Michel-Beyerle, M. E.; Habekorn, R.; Bube, W.; Steffens, E.; Schröder, H.; Neusser, H. J.; Schlag, E. W.; Seidlitz, H. *Chem. Phys.* **1976**, *17*, 139.

(29) (a) Schulten, K.; Staerk, H.; Weller, A.; Werner, H. J.; Nickel, B. *Z. Phys. Chem. N. F.* **1976**, *101*, 371. (b) Treichel, R.; Staerk, H.; Weller, A. *Appl. Phys. B* **1983**, *31*, 15. (c) Weller, A.; Staerk, H.; Treichel, R. *Faraday Discuss. Chem. Soc.* **1984**, *78*, 271. (d) Werner, H.-J.; Staerk, H.; Weller, A. *J. Chem. Phys.* **1978**, *68*, 2419. (e) Staerk, H.; Busmann, H.-G.; Kuhnle, W.; Treichel, R. *J. Phys. Chem.* **1991**, *95*, 1906.

(30) Poulos, A. T.; Kuzmin, V. A.; Geacintov, N. E. *J. Biochem. Biophys. Methods* **1982**, *6*, 269.

(31) Yang, S. K.; McCourt, D. W.; Gelboin, H. V.; Miller, J. R.; Roller, P. P. *J. Am. Chem. Soc.* **1977**, *99*, 5124.

(32) The extinction coefficient of BPT in aqueous solutions was determined by hydrolysis of BPDE (<5 μM, molar extinction coefficient = 2.9 × $10^4$ $M^{-1}$ $cm^{-1}$ at 344 nm, ref 33. No noticeable changes of the BPT absorbances, and therefore molar extinction coefficients, were observed in acetonitrile, DMF, and NMF.

(33) Geacintov, N. E.; Ibanez, V.; Benjamin, M. J.; Hibshoosh, H.; Harvey, R. G. In *Polynuclear Aromatic Hydrocarbons: Formation, Metabolism and Measurement:* Cooke, M., Dennis, A. J., Eds.; Battelle Press: Columbus, OH, 1983; p 559.

**Table 1.** Parameters Characterizing the Photoinduced Electron-Transfer Reactions in Covalently Linked (+)-*trans*-BPDE–DNA, the Covalent BPDE–Native DNA Adduct, and the Noncovalent BPT/dG Solution System

| parameters | BPT + dG | | | (+)-*trans*-BPDE–dG | | BPDE–DNA |
|---|---|---|---|---|---|---|
| | $H_2O$[a] | DMF[b] | NMF[b] | $H_2O$ | DMF | $H_2O$ |
| relative fluorescence yield, $\phi_{f,rel}$ | 0.016[a] | 0.073 | 0.12 | ≤0.006[d] | ≤0.003[d] | 0.05[d] |
| quenching rate constant, $k_q$ ($M^{-1}$ $s^{-1}$) | $2.9 \times 10^9$ | $7.1 \times 10^8$ | $4.1 \times 10^8$ | | | |
| quantum yield of triplet state, $\phi_T$ | 0.09[c] | 0.25 | 0.16 | 0.04 | 0.10 | 0.1 |
| quantum yield of triplet state, $\phi_T$(IS) (expected from intersystem crossing) | 0.008 | 0.029 | 0.048 | 0.003 | 0.0012 | 0.025 |
| quantum yield of radicals, $\phi_R$ | <0.01 | 0.29 | 0.24 | <0.01 | <0.01 | <0.01 |

[a] [dG] = 0.028 M. [b] [dG] = 0.1 M. [c] This value of $\phi_r$ was obtained by fitting eq 5 to the experimental $D_0/D$ vs [dG] plot shown in Figure 3, using values of other parameters measured independently (see text). [d] Upper limit values, since the presence of trace amounts of highly fluorescent BPT decomposition products cannot be excluded.[11e,f]

BPDE–dG adduct absorption maxima occur at 348 nm, probably because of specific solute–solvent interactions. In DMF and NMF, addition of dG does not perturb the fluorescence excitation and emission spectra of BPT, but the fluorescence yields are strongly diminished (next section). In aqueous solutions, the fluorescence and emission spectra of BPT are slightly red-shifted (1–2 nm), particularly at the higher dG concentrations, because of a small but finite fluorescence yield of noncovalent BPT···dG complexes.[15,17a]

**Relative Fluorescence and Triplet Yields.** In the polar organic solvents DMF and NMF, the fluorescence yield ratios $F_0/F$ ($F_0$ and $F$ are the fluorescence signals at 378 nm in the absence and presence of quencher, respectively) increase with increasing dG concentration, and the Stern–Volmer plots are linear up to the highest dG concentrations (0.2 M, data not shown). Values of the bimolecular quenching constants $k_q$ can be determined from these plots, and typical values are listed in Table 1. It is interesting to note that the values of the bimolecular quenching constants $k_q$ for the quenching of the fluorescence of BPT by dG are 4–7 times larger in aqueous solution than in the polar organic solvents DMF and NMF. This effect is attributed to the stronger, noncovalent, hydrophobic interactions between the BPT and dG moieties in the aqueous solvents (see below).

The very low fluorescence yields ($\phi_{f,rel}$) measured relative to those of BPT in aqueous, DMF, and NMF solutions of BPDE–dG adducts (Table 1) are due to the highly efficient intramolecular quenching of the pyrenyl singlet excited state by the dG moiety. With the assumption that the small fluorescence yield ($\phi_{f,rel}$) of the BPT···dG complexes can be neglected[15] and with excitation at an isosbestic point, the following equation can be used to describe both dynamic and static fluorescence quenching:[34]

$$F_0/F = (1 + K_g[dG])\,(1 + k_q\tau_0[dG]) \qquad (2)$$

The line drawn through the $F_0/F$ data points in Figure 3 is obtained from this equation with values $K_g = 100$ $M^{-1}$, $k_q = 2.9 \times 10^9$ $M^{-1}$ $s^{-1}$, and the singlet excited-state ($^1$BPT) lifetime $\tau_0 = 200$ ns, all of which are close to those measured in the more narrow range[15] of [dG] < 0.01 M. The good fit of eq 2 in a wide range of [dG] lends support to the conclusion that $\phi_{f,rel} \leq 0.01$. According to a simple quenching model in which intersystem crossing to the triplet manifold competes with other nonradiative processes which deactivate the singlet excited state to the ground state, the $F_0/F$ and $D_0/D$ curves in Figure 3 should coincide. Since the $D_0/D$ values are significantly smaller than the $F_0/F$ points, these results indicate that the fluorescence quenching reaction results in the generation of molecular triplet excited states.

Unusually high triplet yields are observed along with strong fluorescence quenching in covalent BPDE–DNA and BPDE–dG adducts and for BPT in the presence of 0.028 M dG, all in aqueous solutions. These are compared in Figure 2. All yields are expressed relative to the fluorescence (100% for the purposes of these calculations) and triplet yields of BPT (absolute yield 0.50 ± 0.05, see below) in aqueous solutions (~1 μM) in the absence of quenchers. In the case of BPDE–native DNA adducts, the fluorescence yield is 20 times lower than for BPT, but the triplet yield is only ~5 times smaller. In aqueous solutions of BPDE–dG adducts, the relative fluorescence yield is only 0.6 ± 0.2%, while the relative triplet yield is over 10 times larger (8%). In aqueous BPT solutions containing 0.028 M dG, the fluorescence is also strongly quenched (1.6% relative yield), while the relative triplet yield is 18% (Figure 2).

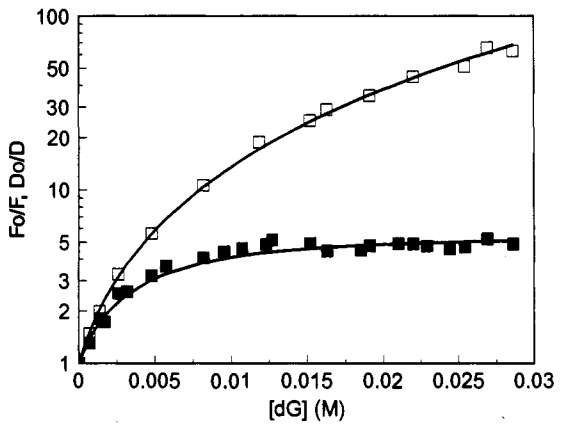


**Figure 3.** Stern–Volmer plots of the fluorescence, $F_0/F$ (□), and triplet yield ratios, $D_0/D$, *vs* the dG concentration in aqueous solutions of BPT. Upper and lower solid lines: plots of eqs 2 and 5, respectively, utilizing the values of the parameters given in Table 1 and in the text; [BPT] = 3 μM (□) and 30 μM (■).

**Transient Absorption Spectra.** Time-dependent absorption spectra of PAH derivatives are often measured using Nd:YAG laser picosecond or nanosecond pulse width excitation using the third harmonic (355 nm). However, the longest-wavelength absorption maximum of BPDE–dG adducts in aqueous solutions is situated at 345 nm, and the molar extinction coefficient drops off rapidly with increasing wavelength, corresponding to less than[2e] ~10% of the maximum value at 355 nm ($\epsilon_{345} = 29\,000 \pm 1000$ $M^{-1}cm^{-1}$). An example of time-dependent absorption spectra following 355-nm excitation with a 10-ns-wide Nd:YAG laser pulse is shown in Figure 4. A rather broad absorbance in the range of 460–520 nm decays with increasing probe flash delay time, and prominent absorptions at 415 and 455 nm as well as at wavelengths to the red of 450 nm manifest themselves at 100 ns and decay within 1 μs. As is shown below, the broad absorbance between 450 and 520 nm is due to singlet excited-state absorption ($S_n \leftarrow S_1$ of the pyrenyl residue), while the 415- and 455-nm maxima are attributed to pyrenyl triplets and pyrenyl radical cations, respectively.

**3.2. Identification of Transient Absorption Spectra.** In this work, both aqueous and nonaqueous solvent systems were used, and various types of transient absorption spectra were observed upon laser pulse excitation at 347 nm. In addition, the nature of the transient absorption spectra depended in some cases on the energies of the laser excitation pulses; representative "high" laser pulse energy spectra were obtained using energies of 20 mJ (~100 mJ/cm²/pulse), while "low" excitation energy spectra were obtained using pulse energies <3 mJ (<15 mJ/cm²/pulse). The absorption characteristics of the BPT pyrenyl residue singlet

(34) Vaughan, W. M.; Weber, W. *Biochemistry* **1970**, *9*, 464.

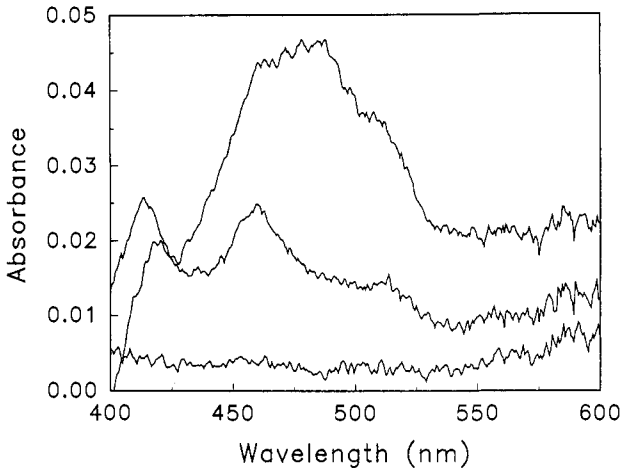


**Figure 4.** Transient absorption spectra of (+)-*trans*-BPDE–dG covalent adduct (5 $\mu$M) in aqueous solution excited with 355-nm laser pulses of high energies (190 mJ/cm$^2$/pulse, 7 ns fwhm). Top transient spectrum: measured at the end of the excitation laser pulse (some of the singlet excited state absorption might be due to traces of BPT decomposition products). Intermediate spectrum: 100 ns after the laser flash. Lowest curve: 5 $\mu$s after the laser flash.

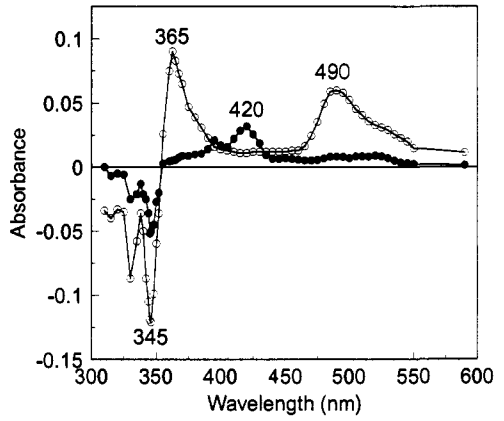


**Figure 5.** BPT (15 $\mu$M) in DMF solution (no quenchers). Transient absorption spectra recorded at various delay times after low-energy laser pulse excitation ($\lambda$ = 347 nm, ~2 mJ/pulse, or 10 mJ/cm$^2$); (○) 10 ns and (●) 1 $\mu$s after the laser flash.

excited state ($S_1$), triplet excited state ($T_1$), radical cation, and radical anion were not known and had to be established, even though these spectra were not expected to differ substantially from those of pyrene.

**Transient Excited Singlet-State ($S_1$) and Triplet ($T_1$) Absorption.** The transient absorption spectra of BPT in DMF recorded 10 ns and 1 $\mu$s after the 347-nm excitation flash (~3 mJ), are shown in Figure 5. In this case, in the absence of electron donors and acceptors, only excited-state singlet–singlet and triplet–triplet absorption spectra are expected. Simultaneously with the appearance of the transient absorption spectra above ~350 nm, a transient bleaching, resembling an inverted absorption spectrum of BPT, appears in the 300–350-nm spectral region which is attributed to ground-state depletion (Figure 5). Similar effects are observed with BPT dissolved in aqueous solutions (data not shown). The kinetic parameters of the recovery of the absorbance at 310–350 nm coincide with those of the decay at 365 nm and in the 450–550-nm regions (singlet lifetimes $\tau_0$ = 180 ± 10 ns in DMF, 200 ± 10 ns in water[35]); thus, the transient absorption maximum at 490 nm and the broad shoulder in the 500–520-nm region are attributed to the singlet–singlet absorption of the $^1$BPT excited state.[36] This transient absorption spectrum resembles the excited singlet-state absorption spectrum of pyrene in cyclohexane,[37] although in that case the maximum in the visible region occurs at 470 nm and not at 490 nm as it does for $^1$BPT. The decay of $^1$BPT is accompanied by a rise in the absorption maximum at 415–420 nm, which is attributed to intersystem crossing with the formation of the triplet excited-state[30] $^3$BPT. The decay of $^3$BPT in oxygen-free solvents occurs on a millisecond time scale, in agreement with previous results.[30] Based on the bleaching of the ground state and the known ground-state molar extinction coefficients,[32] the quantum yields of $^3$BPT formation ($\phi_{T_0}$) in different solvents via intersystem crossing from $^1$BPT can be estimated[38] ($\phi_{T_0}$ = 0.5 ± 0.05 in water and 0.4 ± 0.04 in DMF, NMF, and acetonitrile). In all of the solvents used here, the characteristic triplet–triplet absorption maxima were observed at 415–420 nm, together with a broad absorbance in the 450–530-nm range (Figure 5). In a previous publication from this laboratory, laser photolysis of an aqueous methanol solution of (+)-*trans*-BPDE–dG adduct with picosecond time resolution yielded a transient absorption spectrum with a maximum at 490 nm and a prominent shoulder at[17a] 510 nm; these maxima were erroneously attributed to the pyrenyl residue anion (BPT$^-$ and the dG radical cation, respectively. The previously observed transient absorption spectra agree with the excited singlet absorption spectrum in the same wavelength region as shown in Figure 5. Furthermore, the BPT$^-$ spectrum exhibits a rather sharp absorption maximum at 490 nm and does not exhibit a shoulder at 510 nm (see below).

Finally, a comparison of the photophysical characteristics of BPT (molar extinction coefficients, lifetimes, values of $\phi_{T_0}$) with the known values for pyrene[39–42] indicates that the photophysical properties of BPT in the ground, singlet, and triplet excited states are close to those of the corresponding states of pyrene.[43]

**Formation of the BPT Radical Ions BPT$^{\cdot+}$ and BPT$^{\cdot-}$ via Fluorescence Quenching of $^1$BPT by *N,N'*-Dimethylaniline and Tetracyanoethylene.** The electron donor *N,N'*-dimethylaniline and electron acceptor tetracyanoethylene have been traditionally used to study photoinduced electron transfer and the photochemistry of pyrene.[25] Using low laser pulse energies (≤3 mJ), the radical anions BPT$^{\cdot-}$ and radical cations BPT$^{\cdot+}$ were generated via quenching of the fluorescence of $^1$BPT by these two quenchers, respectively.

(35) This value is the same as the fluorescence decay time of BPT in oxygen-free aqueous buffer solutions.[11e]

(36) Due to specific solvation effects in DMF and NMF, the characteristic transient absorption maxima of $^1$BPT (365 and 490 nm) are shifted to longer wavelengths relative to those in water and acetonitrile (360 and 480 nm). In all of the solvents used in this work, the characteristic $^1$BPT absorption bands centered at 480–490 nm exhibit a characteristic shoulder at 500–520 nm.

(37) Richards, J. T.; West, G.; Thomas, J. K. *J. Phys. Chem.* **1970**, *74*, 4137.

(38) A comparison of the transient absorption and bleaching spectra allows for estimates of the molar extinction coefficients of $^1$BPT (1.6 × 10$^4$ M$^{-1}$ cm$^{-1}$ at 480–490 nm) and of $^3$BPT (2.1 × 10$^4$ M$^{-1}$ cm$^{-1}$ at 420 nm), assuming that the BPT ground-state extinction coefficient[33] at 343–345 nm is 2.9 × 10$^4$ M$^{-1}$ cm$^{-1}$. This procedure should provide correct values of extinction coefficients as long as $^1$BPT and $^3$BPT do not absorb at 343–345 nm. While this seems to be true for $^3$BPT, this is probably not entirely correct for the excited singlet-state $^1$BPT, which absorbs significantly in the 360–365-nm region (Figure 5). Nevertheless, using these procedures, the quantum yields of triplet formation can be estimated.

(39) Porter, G.; Topp, M. *Proc. R. Soc. London, Ser. A* **1970**, *315*, 163.

(40) Post, M. F. M.; Langelaar, J.; Van Voorst, J. D. W. *Chem. Phys. Lett.* **1971**, *10*, 468.

(41) Heinzelmann, W.; Labhart, H. *Chem. Phys. Lett.* **1969**, *4*, 20.

(42) Lavalette, D.; Bensasson, R.; Amand, B.; Land, E. J. *Chem.Phys. Lett.* **1971**, *10*, 331.

(43) The $^1$BPT singlet excited state is strongly quenched by molecular oxygen; in DMF, the corresponding rate constant, $k(O_2)$ = 1.7 × 10$^{10}$ M$^{-1}$ s$^{-1}$ ([$O_2$] = 4.8 × 10$^{-3}$ M in oxygen-saturated DMF, ref 44 a), is close to the diffusion-controlled rate constant for oxygen in nonviscous organic solvents ($k_{diff}$ = (2–3) × 10$^{10}$ M$^{-1}$ s$^{-1}$, ref 44 b). The major product of $^1$BPT quenching by $^3O_2$ is the triplet $^3$BPT, as determined from the fact that the triplet yield $\phi_T$ increases in the presence of oxygen (data not shown), in accordance with analogous previous observations with pyrene.[37] In oxygen-saturated organic solvents, the values of $\phi_T$ in the case of BPT are close to unity (data not shown). Oxygen also reacts with $^3$BPT, stimulating its intersystem crossing to the BPT ground state. The corresponding rate constant is close to $^1/_9 k_{diff}$ because of the spin statistical factor[44b] and, e.g., in dimethylfomamide, $k(O_2)$ = 2.1 × 10$^9$ M$^{-1}$ s$^{-1}$ (see also ref 30).

(44) (a) Landolt-Börnstein. *Zahlenwerte und Functionen*; Springer-Verlag: New York, 1976; Band IV, Tl.4, s.269. (b) Gijzeman, O. L.; Kaufman, K.; Porter, G. J. *Chem. Soc., Faraday Trans. 2* **1973**, *69*, 708.

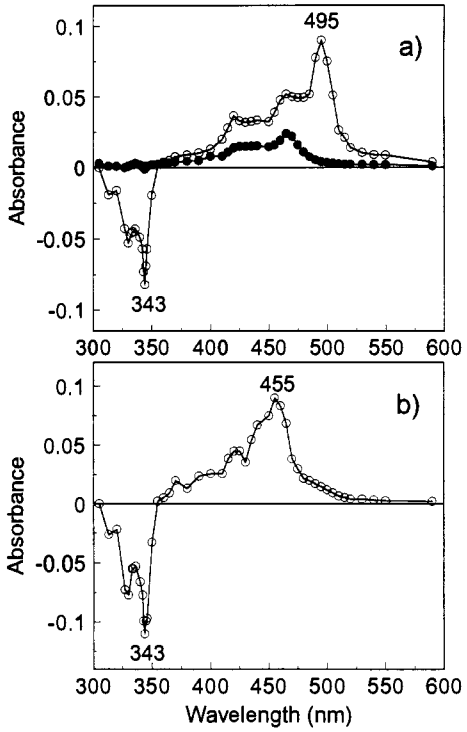


**Figure 6.** BPT (15 $\mu$M) in air-saturated acetonitrile in the presence of fluorescence quenchers: (a) 0.1 M *N,N'*-dimethylaniline, (b) 0.1 M tetracyanoethylene. Transient absorption spectra recorded at various delay times after laser pulse excitation ($\lambda$= 347 nm, low energy ~10 mJ). The spectrum in b was normalized at 455 nm to the spectrum in a at 495 nm. (a) (○) 10 ns and (●) 1 $\mu$s after the laser flash; (b) (○) 10 ns after the laser flash.

The quenching of $^1$BPT by *N,N'*-dimethylaniline is highly efficient; for example, in acetonitrile, the second-order quenching rate constant $k_q$ is equal to $1.6 \times 10^{10}$ $M^{-1}$ $s^{-1}$ (data not shown). The formation of the $BPT^-$ radical anion can be easily traced by its characteristic narrow absorption band at 495 nm in acetonitrile (Figure 6a) or at 500 nm in DMF and NMF (data not shown). In contrast to $^1$BPT, the radical anion $BPT^-$ neither absorbs at 365 nm nor displays a shoulder in the 500–520-nm region; therefore, $^1$BPT and $BPT^-$ can be easily distinguished from one another. In air-saturated acetonitrile solution, the lifetime of $BPT^-$ is equal to 50 ns, much shorter than the lifetime of $^3$BPT (300 ns under the same conditions) as well as the lifetime (>10 $\mu$s) of the radical cation $DMA^{\cdot+}$, derived from the oxidation of *N,N'*-dimethylaniline. These differences provide an opportunity for kinetically separating the transient absorption spectra of all of the transient species. At high *N,N'*-dimethylaniline concentrations ([DMA] > 0.01 M), the $BPT^-$, $^3$BPT, and $DMA^{\cdot+}$ absorption spectra are superimposed immediately after the laser flash (Figure 6a). However, after a 1-$\mu$s delay, only the transient absorption spectrum of the $DMA^{\cdot+}$ cation remains[45] (Figure 6a). Tetracyanoethylene also quenches the fluorescence of $^1$BPT efficiently by electron transfer.[25a] In acetonitrile solution, the corresponding second-order rate constant $k_q$ is equal to $1.8 \times 10^{10}$ $M^{-1}$ $s^{-1}$. At high concentrations of tetracyanoethylene, superimposed transient absorption spectra due to $BPT^{\cdot+}$ ($\lambda_{max}$ = 455 nm, Figure 7) and the reduced tetracyanoethylene anion $TCNE^-$ ($\lambda_{max}$ = 425 nm, ref 46) appear immediately after the excitation flash (Figure 6b). The $BPT^{\cdot+}$ radical cation is characterized by a narrow absorption maximum at 455 nm.

(45) Comparison of the $BPT^-$ and $DMA^{\cdot+}$ transient absorbances allows for an estimate of the $BPT^-$ molar extinction coefficient ($4 \times 10^4$ $M^{-1}$ $cm^{-1}$ at 495 nm, using a value of $4.6 \times 10^3$ $M^{-1}$ $cm^{-1}$ at 470 nm for $DMA^{\cdot+}$, see Zador, E.; Warman, J. M.; Hummel, A. *J. Chem. Soc., Faraday Trans. 1* **1976**, *72*, 1368.).

(46) Liptay, W.; Briegleb, G.; Shindler, K. *Ber. Bunsen-Ges. Phys. Chem.* **1962**, *66*, 331.

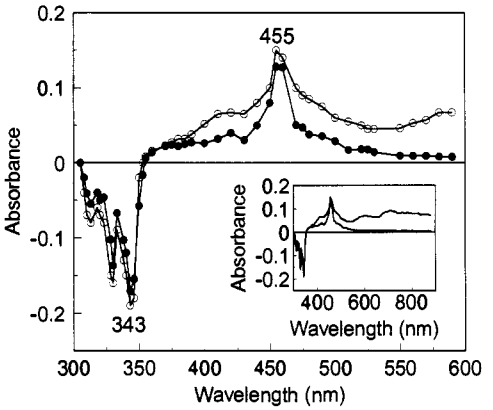


**Figure 7.** BPT (10 $\mu$M) in aqueous solutions. Transient absorption spectra recorded at various times after high-energy (~20 mJ, or 100 mJ/cm$^2$) laser pulse excitation ($\lambda$ = 347 nm). (○) 10 ns and (●) 2 $\mu$s after the laser flash.

Thus, the radical ions $BPT^-$ and $BPT^{\cdot+}$ can be easily generated via the quenching of $^1$BPT by the appropriate electron donors and acceptors. The spectral characteristics of the BPT radical ions are close but not identical to those of the corresponding pyrene radical ions.[47]

**Generation of Pyrenyl Radical Cations at High Laser Pulse Energies.** Regardless of the type of sample, when the laser pulse energy is increased to 20 mJ or more (>100 mJ/cm$^2$/pulse), transient absorption spectra appear with prominent maxima at 455 nm. This effect occurs both in the absence and in the presence of nucleic acids. Typical results obtained with an aqueous solution of BPT (10 $\mu$M) exposed to a 20-mJ laser pulse are shown in Figure 7. A long-lived transient (lifetime ~10 $\mu$s) exhibiting an absorption maximum at 455 nm is identified (by comparison with Figure 6b) as the radical cation $BPT^{\cdot+}$, which is formed by the photoionization of BPT. Another shorter-lived transient (lifetime 0.5 $\mu$s) with a broad absorption spectrum from 480 to 800 nm (see the inset in Figure 7) corresponds to the well-known transient absorption of hydrated electrons with a broad maximum around[48] 700 nm. Comparison of the molar extinction coefficient of hydrated electrons ($1.9 \times 10^4$ $M^{-1}$ $cm^{-1}$ at[49] 700 nm) gives the value of $3.0 \times 10^4$ $M^{-1}$ $cm^{-1}$ for the extinction coefficient of $BPT^{\cdot+}$ at 455 nm.

In the range of laser pulse energies 5–20 mJ (25–100 mJ/cm$^2$/pulse), the yield of hydrated electrons and $BPT^{\cdot+}$ depends on the square of the laser pulse fluence (data not shown). At pulse energies of 20 mJ, only relatively small signals due to $^3$BPT can be discerned, and a small amount of absorbance due to $^1$BPT may also be present though difficult to distinguish even 10 ns after the actinic flash. Efficient photoionization of pyrene to pyrenyl radical cations with a similar absorption spectrum and dependent on the square of 347-nm laser pulse energies has been previously observed in alcoholic solutions of pyrene.[37]

It should be noted that the decay of hydrated electrons is faster than that of $BPT^{\cdot+}$, although the decay of $BPT^{\cdot+}$ results in the regeneration of ground-state BPT molecules (the bleaching of the BPT absorption band at 300–350 nm is reversible). One possible explanation is that $BPT^{\cdot+}$ radical cations recombine with some products of hydrated electron decay.

The formation of $BPT^{\cdot+}$ is also easily observed using laser pulse energies of 20 mJ when BPT is dissolved in the polar organic solvents DMF and NMF; however, the yields of ionization products are much smaller than those observed in water, and the neutral species $^1$BPT and $^3$BPT account for most of the transient absorbance.

(47) (a) Aalsbersberg, W. I.; Hoijtink, G. J.; Mackor, E. L.; Weijland, W. P. *J. Chem. Soc. (London) Part 3* **1959**, 3049. (b) Jagur-Grodzinski, J.; Feld, M.; Yang, S. L.; Szwarc, M. *J. Phys. Chem.* **1965**, *69*, 628.

(48) Hart, E. J.; Boag, J. W. *J. Am. Chem. Soc.* **1962**, *84*, 4090.

(49) Buxton, G. V.; Greenstock, C. L.; Helman, W. P.; Ross, A. B. *J. Phys. Chem. Ref. Data* **1988**, *17*, 2420.

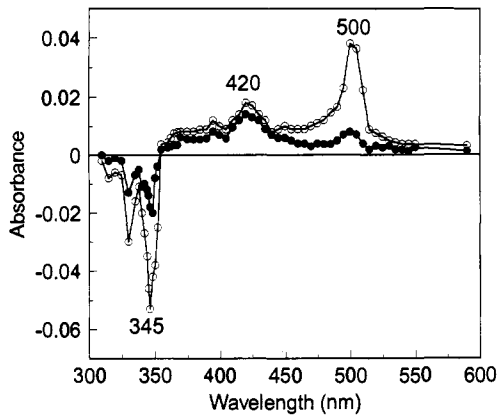


**Figure 8.** BPT (15 $\mu$M) and dG (0.1 M) in DMF solution. Transient absorption spectra recorded at various times after low laser pulse energy (~2 mJ) excitation, $\lambda$= 347 nm). (○) 300 ns and (●) 9 $\mu$s after the laser flash.

In aqueous solutions, high laser pulse energy excitation (20 mJ) of aqueous solutions of BPDE–DNA adducts and BPDE–dG adducts also results in the appearance of the characteristic absorption of solvated electrons and photoionization of the pyrenyl residues to the radical cations. In the range of pulse energies of 5–20 mJ, the yields of radical cations in aqueous solutions of BPDE–dG adducts is 3–4 times lower than those in aqueous solutions of BPT.

**3.3. Laser Flash Photolysis of the Covalent BPDE–dG and Noncovalent BPT/dG Systems: Photoinduced Intermolecular Electron-Transfer Reactions between $^1$BPT and dG in Polar Organic Solvents.** In order to exclude the formation of free-radical ions via photoioniztion, low-level laser pulse excitation (≤3 mJ/pulse) was used for studying the fluorescence quenching interactions between $^1$BPT and dG and the products of this reaction by transient absorption spectroscopy. The lifetimes ($\tau_0$) of $^1$BPT singlets are shortened in the presence of dG and can be monitored either via their fluorescence or via decay of the transient $^1$BPT absorption spectra. The corresponding bimolecular quenching rate constants $k_q$ (Table 1), estimated by either method, are the same within experimental error.

Transient absorption spectra obtained with BPT/dG solutions in DMF measured 300 ns and 9 $\mu$s after the laser flash are shown in Figure 8. Within 300 ns after the actinic flash, a rather sharp absorption band centered at 500 nm is observed. The narrowness of this band, the lack of a shoulder in the 500–520-nm region, and its resemblance to the 500-nm band observed upon the photoreduction of $^1$BPT (Figure 6b) suggest that the quenching of the fluorescence of $^1$BPT by dG in DMF solution is accompanied by the formation of the radical anion BPT$^{\bullet-}$; this is the first unambiguous indication that photoinduced electron transfer is occurring between a benzo[*a*]pyrene metabolite and a nucleic acid base, thus accounting for the efficient fluorescence quenching of $^1$BPT by the nucleic acid base dG. Another absorption maximum is observed at 420 nm and is attributed to the triplet excited-state $^3$BPT. Analogous results were obtained in NMF solution. Thus, we conclude that in DMF and NMF solutions, intermolecular quenching of $^1$BPT by dG results in the formation of BPT$^{\bullet-}$ ($\lambda_{max}$ = 500 nm) and $^3$BPT ($\lambda_{max}$ = 415–420 nm). These events can be summarized as follows:

$$^1\text{BPT} + \text{dG} \longrightarrow [^1\text{BPT}\cdots\text{dG}] \begin{cases} \xrightarrow{a} \text{BPT}^{\bullet-} + \text{dG}^{\bullet+} \\ \xrightarrow{b} {}^3\text{BPT} + \text{dG} \end{cases} \quad (3)$$

where [$^1$BPT···dG] is a collisionally formed intermediate noncovalent excited complex. The transient absorption due to BPT$^{\bullet-}$ disappears more rapidly than that of the triplet $^3$BPT; after 9 $\mu$s, the contribution of $^3$BPT to the overall absorbance is greater than that of BPT$^{\bullet-}$. The appearance of the BPT$^{\bullet-}$ radical anion suggests that the dG radical cation dG$^{\bullet+}$ is also formed as a result of the quenching of $^1$BPT quenching by dG (eq 3). However, neither this radical cation nor its neutral deprotonated form[50] dG(-H)$^{\bullet}$ was observed unambiguously in the transient absorption spectra, most likely because of their small extinction coefficients over a wide range of wavelengths ($\epsilon$ < 2000 M$^{-1}$ cm$^{-1}$ at 350–650 nm, refs 50 and 51).

From the absorbance at 420 nm after a suitable time delay (Figure 8), the relative absorbance due to $^3$BPT triplets was determined as a function of dG concentration. The absolute triplet yield ($\phi_T$) and the quantum yield of radical anions BPT$^{\bullet-}$ ($\phi_R$) were determined by referring to the extent of bleaching at 345 nm as described above. The values of $\phi_T$ and $\phi_R$ in water, DMF, and NMF are compared to one another in Table 1. With BPT dissolved in water or in DMF (NMF), we found that $\phi_{T_0}$ = 0.50 ± 0.05 or 0.40 ± 0.04, respectively, in the absence of any quenchers. In the presence of quenchers and if normal intersystem crossing from the excited singlet state of BPT is the only mechanism of generation of triplets, the triplet yield $\phi_T$(IS) is expected to obey the following relationship:

$$\phi_T(\text{IS}) = \phi_{T_0}(F/F_0) \quad (4)$$

The expected values of $\phi_T$(IS), if generated by a simple intersystem crossing mechanism according to eq 4, are also listed in Table 1. It is evident from Table 1 that the observed triplet yields $\phi_T$ are in all cases much greater than the value of $\phi_T$(IS). For example, in the case of BPT in the presence of 0.028 M dG, the predicted value of $\phi_T$(IS) = 0.008, while the observed value $\phi_T$ is nearly 1 order of magnitude greater (Table 1).

In aqueous BPT/dG solutions, using pulse energies ≤3 mJ (15 mJ/cm$^2$/pulse), neither of the free radical ion species BPT$^{\bullet-}$ or BPT$^{\bullet+}$ was observed, and only triplet excited states $^3$BPT manifest themselves even at the shortest feasible delay times (~10 ns). The sole products of the quenching of the fluorescence of $^1$BPT by dG are ground-state BPT and $^3$BPT triplets according to the scheme in eq 3b.

The triplet yield ratio $D_0/D$ ($D_0$ and $D$ are absorbencies of $^3$BPT at 420 nm in the absence and presence of dG, respectively) is less than $F_0/F$, in accordance with the relationship $\phi_T > \phi_T$(IS), since $D_0/D \approx F_0/F$ in the case $\phi_T \approx \phi_T$(IS). It is evident from Figure 3 that the deviation of $D_0/D$ from $F_0/F$ is especially pronounced at high dG concentrations. These differences between the $D_0/D$ and $F_0/F$ values strongly suggest that another mechanism besides normal intersystem crossing is responsible for the enhanced triplet yields. These alternate routes include $^3$BPT formation via dynamic (intermolecular) quenching and static (intramolecular) quenching of $^1$BPT via the formation of noncovalent (BPT···dG) complexes. The following equation for the triplet yield ratio was obtained by assuming that the $\phi_T$ values are close to one another for these two quenching pathways and formation of $^3$BPT:

$$D_0/D = \frac{1 + K_g[\text{dG}]}{(1 + \phi_{T,rel}k_q\tau_0[\text{dG}])/(1 + k_q\tau_0[\text{dG}]) + \phi_{T,rel}K_g[\text{dG}]} \quad (5)$$

where $\phi_{T,rel}$ is the relative triplet yield, $\phi_T/\phi_{T_0}$. The line drawn through the $D_0/D$ data points in Figure 3 is a fit of eq 8 to the experimental results. The value of $\phi_{T,rel}$ = 0.18 (Figure 2) was the only adjustable parameter since the values of $K_g$, $k_q$, and $\tau_0$ were measured independently and were the same as those used to construct the $F_0/F$ plot in Figure 3. Table 1 shows that the $\phi_T$ values in the quenching of the fluorescence of $^1$BPT by dG is 2–2.5 times smaller in aqueous solution than in the polar organic solvents DMF and NMF.

(50) Candeias, L. P.; Steenken, S. *J. Am. Chem. Soc.* **1989**, *111*, 1094.
(51) Kasama, K.; Takematsu, A.; Arai, S. *J. Phys. Chem.* **1982**, *86*, 2420.

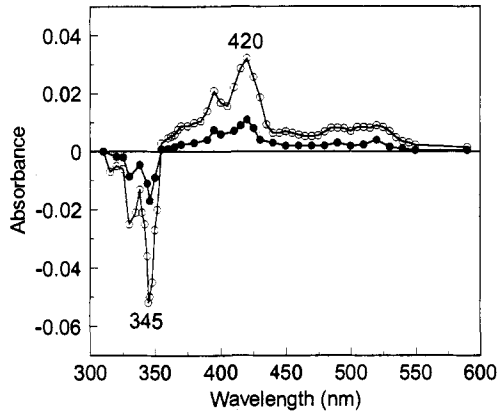


**Figure 9.** Covalent (+)-*trans*-BPDE–dG (15 $\mu$M) and reference BPT (26 $\mu$M) with the same absorbance at 347 nm in DMF solutions. Transient absorption spectra recorded at various times after excitation with low energy (~2 mJ, or 10 mJ/cm$^2$) laser pulses ($\lambda$= 347 nm). (●) 10 ns, BPDE–dG adduct, and (○) 1 $\mu$s, BPT, after the laser flash.

**Enhancement of Triplet Formation in Covalent BPDE–DNA and BPDE–dG Adducts.** In contrast to the observations with solutions of BPT and dG in DMF (Figure 8), radical ions are not observed upon photoexcitation of the covalent BPDE–dG adducts in the same solvent (Figure 9); at a delay time of 10 ns, the absorption spectrum is characterized by a maximum at 415–420 nm and a broad absorption band in the 450–550-nm region (open circles), which is comparable to the transient absorption due to triplet excited states of a BPT solution in DMF, measured 1 $\mu$s after the excitation flash (closed circles). Similar results are obtained with covalent BPDE–DNA adducts and BPDE–dG adducts in aqueous solutions at low laser pulse energies (≤3 mJ), since triplet excited states are the sole products which contribute to the transient absorption spectra within the response time (~10 ns) of the apparatus following photoexcitation (data not shown). The relative yields of triplets in aqueous solutions are significantly greater than expected from the large reductions in the fluorescence yields (Figure 2), and $\phi_T > \phi_T$(IS) in all cases (Table 1). All of these findings are consistent with the existence of an alternative route, besides normal intersystem crossing, for the formation of triplet states of the pyrenyl moieties in the different covalent adducts.

In Table 1, the absolute quantum yields of triplets were calculated from the corresponding $\phi_{T,rel}$ values (Figure 2). In aqueous solutions, $\phi_T$ for the BPDE–DNA adduct is close to the triplet yield observed in the case of BPT in the presence of 0.028 M dG, whereas $\phi_T$ for the BPDE–dG adduct is ~2 times less. However, since there is a heterogeneity of covalent lesions in the BPDE–native DNA adducts, such comparisons of $\phi_T$ are not likely to have quantitative significance in that case. The efficiency of triplet formation for the BPDE–dG adduct is 2.5 times greater in DMF than in water.

## 4. Discussion

**Observation of Ionic Pyrenyl Species Depends on Experimental Conditions.** In all cases, especially in aqueous solutions, excitation of the samples at 347 nm with pulse fluences > 100 mJ/cm$^2$ produces pyrenyl cations with characteristic absorption maxima at 455 nm. Similarly, upon excitation at the tail of the pyrenyl absorption band at 355 nm (190 J/cm$^2$/pulse), a similar transient spectrum with a 455-nm peak also appears (Figure 4). The formation of pyrenyl radical cations is observed even with BPT alone, dissolved in polar solvents, is dependent on the square of the pulse fluence (data not shown) and thus can dominate transient absorption spectra when high-energy laser pulse energies are utilized. The results shown in Figure 4, obtained by excitation with intense 355-nm laser pulses at the tail of the BPDE absorption maximum, are an example of this behavior. Richards and co-workers[37] have concluded that photoionization of pyrene in alcoholic solutions occurs via a direct two-photon absorption from the ground state upon excitation at 347 nm. However, in our case, a tandem singlet excited absorption mechanism cannot be excluded. Two-photon ionization has been also observed for many other polycyclic aromatic hydrocarbons.[52] The main argument for this mechanism is that quenchers ($^3O_2$ or $CH_3I$), which make the lifetime of the singlet excited state shorter than the width of the laser pulse, have no effect on the yield of radical cations.[37] In agreement with this mechanism, in aqueous solutions the yields of radical cations are similar for BPT and BPDE–dG adducts. These effects were not further investigated here.

**Photoinduced Electron Transfer.** Highly efficient quenching of the pyrenyl fluorescence has been observed in BPDE–DNA adducts,[12] in covalently linked BPDE–dG adduct model systems, and as a result of the noncovalent interactions between BPT and the nucleoside dG (Figure 2). At low 347-nm laser pulse fluences (≤6 mJ/cm$^2$/pulse), pyrenyl radical cations are not observed in any of the samples studied here. Instead, the major products of the strong fluorescence quenching reaction (detected on nanosecond time scales) are pyrenyl triplet excited states and, in some cases, pyrenyl residue radical anions. The latter have been observed only in solutions of BPT and dG in the polar organic solvents DMF and NMF.

The thermodynamic driving force $\Delta G$ (eV) for photoinduced electron-transfer reactions between pyrenyl singlet excited states with electron donors (D) and electron acceptors (A) can be roughly estimated from the Rehm–Weller equation:[53]

$$\Delta G = E^\circ(D/D^{\bullet+}) - E^\circ(A/A^{\bullet-}) - \Delta E_{00} - w \qquad (6)$$

Using the known redox potentials of pyrene[54] ($E^\circ$(Py/Py$^-$) = −2.09 V, $E^\circ$(Py$^{\bullet+}$/Py) = 1.28 V vs SCE in DMF) and assuming that the $E^\circ$ values of the pyrenyl residues in BPT or the covalent adducts are not too different from one another, the values of $\Delta G$ can be estimated. The zero–zero transition energy[55] $\Delta E_\infty$(BPT) = 3.28 eV, and the Coulombic ion interaction term $w$ is negligible in polar media ($w$ < 0.1 eV, ref 56). Electron transfer is thermodynamically favorable for electron donor/acceptor pairs with $E^\circ(D/D^{\bullet+}) < 1.19$ V and $E^\circ(A/A^-) > -2.0$ V vs SCE. Indeed, the corresponding radical anions and cations are easily observed in the quenching of the fluorescence of $^1$BPT by the electron acceptors *N*,*N*′-dimethylaniline (DMA) and tetracyanoethylene (TCNE) in acetonitrile solutions in which $E^\circ$(DMA$^{\bullet+}$/DMA) = 0.76 V and $E^\circ$(TCNE/TCNE$^-$) = 0.24 V vs SCE.[57,58]

The oxidative quenching of $^1$BPT by dG with the formation of the radical cation BPT$^{\bullet+}$ is thermodynamically unfavorable ($E^\circ$(dG/dG$^-$) < −2.7 V vs SCE in DMF[20]). However, reductive quenching is observed experimentally at least in the polar solvents DMF and NMF and thus appears to be thermodynamically favored. Unfortunately, in the case of dG, the exact value of $E^\circ$(dG$^{\bullet+}$/dG) is not known since dG exhibits irreversible oxidation in aqueous[18] and aprotic media.[20] For example, in DMF, only the anodic peak potential ($E_{pa}$ = 1.18 V vs SCE) was measured by cyclic voltammetry.[20] The irreversible oxidation of dG is due to the rapid deprotonation of dG$^{\bullet+}$ with formation of the neutral radical[50] dG(-H)$^\bullet$. Measurements of the redox potential of dG by conventional electrochemical techniques gave only crude

(52) For example: (a) Hirata, Y.; Mataga, N. *J. Phys. Chem.* **1985**, *89*, 4031. (b) Scott, T. W.; Albrecht, A. C. In *Advances in Laser Spectroscopy*; Geretz, B. A., Lombardi, J. R., Eds.; Heyden: London, 1982; p 55. (c) Liu, A.; Loffredo, D. M.; Trifunac, A. D. *J. Phys. Chem.* **1993**, *97*, 3791.

(53) Rehm, D.; Weller, A. *Isr. J. Chem.* **1970**, *8*, 259.

(54) Kubota, T.; Kano, J.; Uno, B.; Konse, T. *Bull. Chem. Soc. Jpn.* **1987**, *60*, 3865.

(55) The observed vibronic BPT transition with a maximum at 345 nm is due to the $S_2 \leftarrow S_0$ transition, while the $S_1 \leftarrow S_0$ transition threshold of BPT occurs near 378 nm, and $\Delta E_{00}$ = 3.28 eV.

(56) Bolton, J. R.; Archer, M. D. In *Electron Transfer in Inorganic, Organic, and Biological Systems*; Bolton, J. R., Mataga, N., McLendon, G., Eds.; Advances in Chemistry Series 228; CSC Symposium Series 2; American Chemical Society: Washington, DC, 1991; p 7.

(57) Zweig, A.; Lancaster, J. E.; Neglia, M. T.; Jura, W. H. *J. Am. Chem. Soc.* **1964**, *86*, 4130.

(58) Peover, M. E. *Trans. Faraday. Soc.* **1962**, *58*, 2370.

estimates of $E°(dG^{\cdot+}/dG)$. The redox potential for the dG(-H)$^{\cdot}$/dG(-H)$^{-}$ redox pair was determined in aqueous solutions (pH 13) by pulse radiolysis from electron-transfer equilibria involving dG(-H)$^{\cdot}$ and other free radicals with known redox potentials.[59] Recalculation from $E°$[dG(-H)$^{\cdot}$/dG(-H)$^{-}$] = 0.47 V vs SCE[59] and the corresponding p$K_a$ values[50] for dG (p$K_a$ = 9.4) and dG(-H) (p$K_a$ = 3.9) gives an estimated value of $E°$(dG/dG$^{\cdot+}$) = 0.79 V vs SCE. This estimate of the oxidation potential of dG indicates that electron transfer from dG to $^1$BPT is indeed thermodynamically favorable. In this work we have found the first unambiguous evidence for the formation of radical anions in the quenching of $^1$BPT by dG, with quantum yields of 0.29 in DMF and 0.24 in NMF (Table 1). Interestingly, radical anions were not detected in aqueous solutions either with this noncovalent BPT/dG quenching system or with covalent BPDE–DNA or BPDE–dG adducts. In contrast to the noncovalent fluorescence quenching interactions between $^1$BPT and dG, no pyrenyl radical anions can be detected in the covalent BPDE–dG adduct system in DMF (or NMF) (Table 1).

**Differences between Aqueous and Nonaqueous Solvents.** Differences in the solvent polarity ($\epsilon_{DMF}$ = 36.7, $\epsilon_{NMF}$ = 185) do not seem to significantly affect the magnitude of the second-order $^1$BPT/dG quenching constant $k_q$ nor the quantum yield of BPT$^{-}$ radical anions (Table 1). The lack of a solvent polarity effect on the rates of fluorescence quenching and quantum yields of radical ion formation in polar organic solvents with dielectric constants $\epsilon_s > 30$ is not unexpected from the point of view of electron-transfer theory and is also absent in noncovalent pyrenefluorophore–aromatic amine quenching systems[27] and in covalently linked systems of this type.[60]

The polarity of water ($\epsilon_{aq}$ = 80) is intermediate in value between the polarities of DMF and NMF, but BPT$^{-}$ anions are not observed in aqueous solutions and the value of $k_q$ is 4–7 times larger than in these two polar organic solvents (Table 1). Therefore, some effect other than solvent polarity must account for these differences.

This seemingly anomalous behavior in aqueous solutions is most likely related to the specific interactions between BPT and dG which unambiguously manifest themselves in terms of ground-state complex formation between BPT and dG. These hydrophobic interactions lead to ground-state complex formation between BPT and dG and red-shifted absorption and fluorescence excitation spectra.[15] In the polar organic solvents DMF and NMF, such ground-state complexes are not formed and there is no change in the BPT absorption and fluorescence excitation spectra even at the highest dG concentrations employed (0.2 M). Of course, complex formation between the excited states $^1$BPT and dG can also occur (equilibrium constant $K$), and $K$ should be greater than $K_g$ because of the greater dipole moment in the excited state than in the ground state.[14a] The effects of these hydrophobic interactions on electron transfer and on the observed bimolecular quenching constant $k_q$ may be understood in terms of the scheme shown in eq 7:

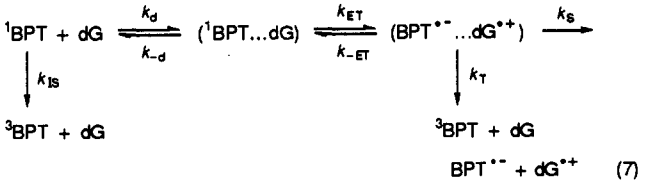

(7)

where $k_d$ and $k_{-d}$ are the rate constants of encounter between $^1$BPT and dG and dissociation, respectively, with $K = k_d/k_{-d}$; $k_{ET}$ and $k_{-ET}$ are the rate constants of charge separation and charge recombination, respectively, while $k_S$ and $k_T$ are the rate constants for ion solvation and triplet formation via the electron-transfer pathway, respectively. The normal intersystem crossing rate constant is denoted by $k_{IS}$. The return of all excited states to the ground state is not shown explicitly.

We note that in water the value of $k_q$ is close to the diffusion-controlled value for two relatively large molecules of this size.[61] In general,[62] in the limits of $k_S + k_T \gg k_{-ET}$ and $k_{-d} \gg k_{ET}$, $k_q \approx Kk_{ET}$. Whenever $k_{ET} \gg k_{-d}$, the observed quenching constant $k_q$ approaches the diffusion-controlled value $k_d$. In aqueous solutions, the latter case is likely to be prevalent because $k_q$ is close to the value of $k_d$. In polar organic solvents, the collisions between $^1$BPT and dG are less "sticky" than in water, implying that the dissociation rate constant $k_{-d}$(water) < $k_{-d}$(DMF, NMF). Thus, complex formation between $^1$BPT and dG is significantly diminished in the organic solvents (decrease in $K$), and $k_q$, the bimolecular rate constant for fluorescence quenching, is thus also diminished (Table 1).

The rate constant of escape of the radical ions into the bulk solution is expressed by the rate constant $k_S$. In water, the specific noncovalent interactions between the BPT$^{-}$ and dG$^{\cdot+}$ radical ions might also diminish the value of $k_S$, thus limiting the escape of ions from one another into the bulk of the solution. This effect might be responsible for the observation that BPT$^{-}$ radical ions are observed only in organic media but not in aqueous solutions.

The high value of $k_q$ in the aqueous BPT/dG system suggests that the forward electron transfer between the pyrenyl and guanosyl moieties in the covalently linked BPDE–dG adducts should be very efficient relative to the intrinsic decay rate of $^1$BPT in the absence of quenchers ($\tau_0^{-1} = 5 \times 10^6$ s$^{-1}$), as is indeed observed (the fluorescence decay rate constant of BPDE–dG adducts is[17b] $\sim 6 \times 10^8$ s$^{-1}$). These decay rates are consistent with the low fluorescence yield of BPDE–dG adducts in aqueous solutions (Table 1). Furthermore, because the ion pair cannot dissociate in the covalent adducts, charge recombination should be more efficient than in the noncovalent BPT/dG system. Indeed, the yield of radical ions is negligible both in aqueous and in nonaqueous systems in the case of covalently linked BPDE–dG moieties.

**Other Mechanisms of Fluorescence Quenching.** An alternative mechanism of fluorescence quenching can include photoinduced electron transfer accompanied by hydrogen abstraction from dG. This type of mechanism was recently proposed by Atherton and Harriman[63] for fluorescence quenching of methylene blue by guanine residues in the synthetic polynucleotide poly(dG-dC). Okada[64] and co-workers provided unambiguous evidence for hydrogen atom transfer in pyrene–amine fluorescence quenching systems. Hydrogen atom abstraction plays a dominant role in the quenching of the fluorescence of pyrene by primary and secondary amines with free N–H groups in nonpolar or weakly polar media. The relative contribution of this mechanism decreases with increasing solvent polarity, and the electron-transfer pathway of fluorescence quenching dominates in polar solvents ($\epsilon_s > 30$). Since dG also contains free N–H groups, the hydrogen atom-transfer mechanism could play a role in the quenching of the fluorescence of BPT in solvents of low polarity ($\epsilon_s < 30$) according to this model.[64] However, investigations along these lines were beyond the scope of this work.

**Enhancement of the Yield of $^3$BPT Triplets.** In view of the pronounced quenching of the pyrenyl singlet excited states, the yields of triplet excited states are unusually high in both the

(59) Jovanovich, S. V.; Simic, M. G. *J. Phys. Chem.* **1986**, *90*, 974.
(60) (a) Heitele, H.; Finckh, P.; Weeren, S.; Pöllinger, F.; Michel-Beyerle, M. E. *J. Phys. Chem.* **1989**, *93*, 5173. (b) Heitele, H.; Pöllinger, F.; Weeren, S.; Michel-Beyerle, M. E. *Chem. Phys. Lett.* **1990**, *168*, 598. (c) Heitele, H.; Pöllinger, F.; Weeren, S.; Michel-Beyerle, M. E. *Chem. Phys.* **1990**, *143*, 325.
(61) Lakowicz, J. R. *Principles of Fluorescence Spectroscopy;* Plenum Press: New York, 1983.
(62) (a) Marcus, R. A. *Int. J. Chem. Kinet.* **1981**, *13*, 865. (b) Marcus, R. A.; Siders, P. *J. Phys. Chem.* **1982**, *86*, 622. (c) Marcus, R. A. *Faraday Discuss. Chem. Soc.* **1982**, *74*, 7.
(63) Atherton, S. J.; Harriman, A. *J. Am. Chem. Soc.* **1993**, *115*, 1816.
(64) (a) Okada, T.; Mori, T.; Mataga, N. *Bull. Chem. Soc. Jpn.* **1976**, *49*, 3398. (b) Okada, T.; Tashita, T.; Mataga, N. *Chem. Phys. Lett.* **1980**, *75*, 331. (b) Okada, T.; Karaki, I.; Mataga, N. *J. Am. Chem. Soc.* **1982**, *104*, 7191.

noncovalent BPT/dG and the covalent adduct systems both in aqueous and in polar organic media (Figure 2 and Table 1). In all cases, formation of the triplet states is observed immediately after the laser flashes on nanosecond time scales, i.e., triplets are formed as a result of primary photochemical reactions and are not connected with subsequent, slower intermolecular recombination of free radical ions. This "fast" triplet formation is a characteristic feature of pyrene photochemistry and has been observed in many pyrene–amine fluorescence quenching systems.[26,29,65,66] Recently, Hashimoto[67] reported that several purine derivatives (specifically, xanthine and uric acid derivatives) also efficiently quench the fluorescence of pyrene and that the triplet yield is enhanced via the decay of intermediate exciplexes, analogous to the fast triplet formation described previously.[26,29,65,66]

The most likely mechanism of fast triplet formation involves the geminate recombination of radical ion pairs resulting in the formation of molecular triplet excited states.[26,29,65,66] An important and obvious requirement of this mechanism is that the energy of the radical ion pair must be greater than that of the triplet excited state. This requirement is easily met by the BPDE–dG adduct system since the energy of the BPT triplet excited state[68] ($E_{00}$ = 2.1 eV) is lower than that of the initially born radical ion pair[69] (E ≈ 2.9 eV). Since the radical ion pairs are born with overall singlet multiplicity, intersystem crossing to the triplet manifold must precede ion pair recombination.

Two alternative mechanisms of intersystem crossing involving charge-separated states as intermediates can be defined. These mechanisms are summarized in the following scheme:

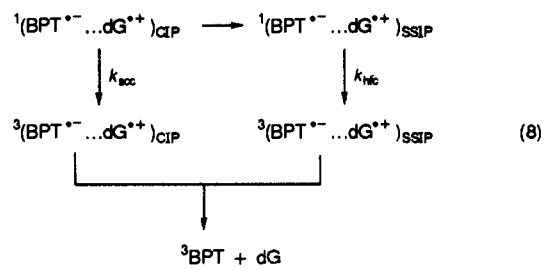


For simplicity, we define two limiting cases of radical ion pairs in solution. In the first, a short-lived species called a contact ion pair (CIP), the radical cation and anion are assumed to be in contact with one another without intervening solvent molecules;[70] here we broaden this definition somewhat by assuming that in this kind of short-lived CIP some solvent molecules may be interspersed between the two radical ions, but the distance between the two radical ions is sufficiently small to allow for a large exchange interaction and thus small singlet–triplet mixing by hyperfine coupling effects.[71] The CIP is formed via intramolecular electron transfer in the exciplex formed from the $^1$BPT···dG encounter complex or directly by excitation of BPT···dG ground-state complexes (for simplicity, these pathways have been omitted in eq 8). In the second limiting case, the ion pairs are sufficiently separated and individually solvated so that the exchange interaction is small; this solvent-separated ion pair[70] (SSIP) formed by dissociation of the CIP or directly by intramolecular electron transfer in $^1$BPT···dG encounter complexes (this pathway is not shown in eq 8), is long-lived (>1 ns) so that triplet–singlet mixing by the hyperfine coupling effect becomes feasible.

Singlet–triplet transitions induced by electron–nuclear hyperfine coupling effects (rate constant $k_{hfc}$) have been studied extensively in pyrene–aromatic amine systems.[28,29] This mechanism of intersystem crossing is efficient in relatively long-lived radical ion pairs (SSIP) because the singlet–triplet transitions induced by the hyperfine coupling requires a few nanoseconds ($k_{hfc}$ is equal to $\sim 10^8$ s$^{-1}$ for many organic radicals[71]); the signature of this mechanism is the effect of external magnetic fields on the yield of triplet excited states.[71] The efficiency of the singlet–triplet transitions by this mechanism rapidly decreases with the enhancement of the exchange interaction between unpaired electrons and becomes negligible in CIP states in which exchange interaction is greater than the hypefine coupling.

In short-lived CIP or exciplex states, singlet–triplet transitions are induced by an ultrafast spin–orbit coupling mechanism (rate constant $k_{SOC}$), and triplet excited states are generated on picosecond time scales.[66] In this mechanism, the intersystem crossing rate is enhanced by charge-transfer states and occurs even in the absence of heavy atoms or other paramagnetic species,[72] and the triplet yields do not depend on external magnetic fields. Mataga[66] and co-workers have speculated that ultrafast intersystem crossing from singlet to triplet excited states on picosecond time scales, observed in several noncovalent and covalently linked pyrene–aromatic amine fluorescence quenching systems, is strongly dependent on the relative orientations of the donor–acceptor aromatic ring systems. This intersystem crossing is induced by a spin–orbit coupling mechanism which is anisotropic in nature, which decreases rapidly with increasing distance between ion pairs, and which may thus play an important role in ultrafast triplet formation from short-lived CIP states in which the two radical ions are physically close to one another (separated by at most a few solvent molecules). Such intermediate bimolecular photoexcited contact ion pair states can occur both in noncovalent and in covalently linked donor–acceptor pairs of the type studied in this work.

The relative importance of these two mechanisms can be investigated by studying the effects of magnetic fields on yields of triplet excited states and radical ions; experiments along these lines are presently underway.

## Concluding Remarks

A photoinduced electron-transfer mechanism can account for the efficient quenching of the fluorescence of benzo[*a*]pyrene metabolite model compounds and their derivatives in noncovalent complexes with DNA and with the nucleoside dG and in covalent DNA and dG adducts. Using noncovalent fluorophore/dG mixtures and covalent BPDE–dG adducts dissolved in aqueous and polar organic media as model systems, an enhanced yield of triplet excited states is observed on nanosecond time scales, but pyrenyl radical ions are detected only in polar organic solvents. Noncovalent hydrophobic interactions, which are particularly pronounced in aqueous solutions, can play a significant role in determining the magnitude of the fluorescence quenching constants and limit the escape of radical ions into the bulk of the solution. Thus, in aqueous solutions in general, as well in the covalently linked BPDE–dG and BPDE–DNA adducts in particular, the intermediate radical ion pairs do not separate efficiently, and pyrenyl radical anions are not observed on time scales > 10 ns after the actinic flashes.

**Acknowledgment.** This work was supported by Grant DE-FGO-86ER06045 from The Office of Health and Environmental Research, The U.S. Department of Energy.

(65) Bell, I. P.; Rodgers, M. A. J. *Chem. Phys. Lett.* **1976**, *44*, 249.
(66) (a) Mataga, N.; Migita, M.; Nishimura, T. *J. Mol. Struct.* **1979**, *47*, 199. (b) Okada, T.; Karaki, I.; Matsuzava, E.; Mataga, N.; Sakata, Y.; Mizumi, S. *J. Phys. Chem.* **1981**, *85*, 3957. (c) Mataga, N. *Radiat. Phys. Chem.* **1983**, *21*, 83.
(67) Hashimoto, S. *J. Phys. Chem.* **1993**, *97*, 3662.
(68) Kolubaev, V.; Brenner, H. C.; Geacintov, N. E. *Biochemistry* **1987**, *26*, 2638.
(69) Estimated from the $E°(Py/Py^-)$ = −2.09 V and $E°(dG/dG^+)$ = 0.79 V values discussed earlier.
(70) Asahi, T.; Mataga, N. *J. Phys. Chem.* **1991**, *95*, 1956.
(71) *Spin Polarization and Magnetic Effects in Radical Reactions*; Molin, Yu. N., Ed.; Elsevier: Amsterdam, 1984.
(72) McGlynn, S. M.; Azumi, T.; Kinoshita, M. *Molecular Spectroscopy of the Triplet State*; Prentice Hall: Engelwood Cliffs, 1969; pp 284–325.